Received 9 December 2018; revised 21 March 2019; accepted 7 April 2019. Date of publication 17 April 2019; date of current version 19 August 2019. The review of this paper was arranged by Editor T.-Y. Chu.

Digital Object Identifier 10.1109/JEDS.2019.2910748

Controlling the Surface Properties of an Inkjet-Printed Reactive Oxygen Species Scavenger for Flexible Bioelectronics Applications in Neural Resilience

ASHKAN SHAFIEE [1], ELHAM GHADIRI [1,2,3], MUHAMAD MAT SALLEH [4], MUHAMMAD YAHAYA [4], AND ANTHONY ATALA [1]

1 Wake Forest Institute for Regenerative Medicine, Wake Forest School of Medicine, Winston-Salem, NC 27101, USA
2 Department of Chemistry, Wake Forest University, Winston-Salem, NC 27109, USA
3 Comprehensive Cancer Center, Wake Forest School of Medicine, Winston-Salem, NC 27101, USA
4 Institute of Microengineering and Nanoelectronics, National University of Malaysia, Bangi 43600, Malaysia

CORRESPONDING AUTHOR: A. SHAFIEE (e-mail: ashafiee@wakehealth.edu)

ABSTRACT Neural damage caused by reactive oxygen species (ROS) can trigger several acute or chronic conditions, such as Alzheimer's, Huntington's, and Parkinson's diseases. However, ROS scavengers hold great promise for enabling DNA repair in neurons; damaged cells using ROS-scavenging agents may be able to recover their functionality and resilience. Moreover, in bioelectronics for neural applications, thin films with adequate properties are crucial for the proper performance of an electronic device. Therefore, precise and reliable deposition techniques that can control the characteristics of thin films are imperative when fabricating bioelectronic devices integrated with cellular systems. To that end, inkjet printing is a promising method with unique advantages, such as computer-assisted protocols and efficient consumption of materials. We report the printing of a functional electronic material that exhibits ROS scavenging behavior (Manganese [III] 5, 10, 15, 20-tetra [4-pyridyl]-21H, 23H-porphine chloride tetrakis [methochloride]) using a modified inkjet printer. Different printed pattern schemes that were designed based on the amount of overlap among sequential droplets were used to tune the surface morphology of the inkjet-printed thin films with a wide range of roughness (8.84–41.20 nm). Furthermore, post-printing processes (such as plasma treatment) were used to optimize surface energy. Such inkjet printing methods of functional electronic materials that can simultaneously be used as ROS scavengers, would advance bioelectronics applications in neural studies.

INDEX TERMS Inkjet printing, neural damage, reactive oxygen species scavenger.

I. INTRODUCTION

Reactive oxygen species (ROS) may damage neural cells and elicit several acute or chronic conditions such as Alzheimer's, Huntington's, and Parkinson's diseases [1], [2]. On the other hand, ROS scavengers are ideal candidates for enabling DNA repair in neurons [1], [2]. Damaged cells using ROS scavenging agents may be able to recover their functionality and resilience. Furthermore, such agents could even prevent DNA damage caused by oxidative stress [2]. Moreover, in bioelectronics, the surface properties of thin films may influence the device performance [3], [4]. In flexible bioelectronics for neural applications, thin films with adequate properties are crucial for the proper performance of devices, such as biosensors [5]. Therefore, precise and reliable deposition techniques that can control the characteristics of thin films are imperative when fabricating electronic devices integrated with cellular systems. To that end, inkjet printing is a promising method with unique advantages, such as computer-assisted protocols and efficient consumption of materials [6]–[8]. Printers have been used extensively in

diverse fields ranging from printed electronics [9]–[11] to drug delivery [12] and tissue engineering [13]–[17]. Printed electronics is a relatively new approach to manufacturing electronic devices that incorporate flexible, stretchable, and portable electronics. Fabrication of organic electronic devices such as organic light-emitting diodes and organic solar cells encompasses material selection [18] and precise thin film deposition [19], [20]. Materials used in device fabrication must fulfill some criteria including enhanced semiconductor properties (e.g., appropriate optoelectronic properties such as electrical conductivity and energy level position) in order to build a reliable final product [21], [22]. Different sophisticated characterization techniques including steady state optical spectroscopy, ultrafast laser spectroscopy [23] and electrochemical measurements [18] have been used to determine material optoelectronic properties for optimized device fabrication. Moreover, the properties of organic thin films play essential roles in the quality and performance of organic devices [24]. Thin films' quality strongly impact on the device final performance used in different application. Therefore, a versatile deposition technique with the ability to control the characteristics of thin films is necessary for high quality device fabrication [25].

Drop-on-demand inkjet printers are mostly used in research where economic consumption of materials and accuracy is crucial [26]–[28]. Piezoelectric and thermal printers are two of the most popular drop-on-demand printers and have been used extensively in research. However, the costs may be high and they lack the ability to control the surface morphology.

We report the printing of a functional electronic material that exhibits ROS scavenging behavior using an office inkjet printer. Manganese (III) 5, 10, 15, 20-tetra (4-pyridyl)-21H, 23H-porphine chloride tetrakis (methochloride) was used as both an organic porphyrin dye and a ROS scavenger. This material can be used to fabricate electronic devices while repairing damaged cells by oxidative stress. To control the final film surface roughness, we employed different ink pattern schemes. In the printing process, drops can be deposited using both non-interlaced or interlaced schemes; the difference is in the time allowed for the material to spread and dry before the next drop or line is printed [29]. We successfully tuned the surface properties such as roughness using different schemes (8.84 to 41.20 nm). To the best of our knowledge, this is the first modified, inexpensive inkjet printing system with the ability to control the surface roughness of the films. The hardware reengineering enabled to employ an office inkjet printer as a sophisticated printing deposition apparatus. And software design, using ink pattern schemes, provided a platform to control the surface roughness. Furthermore, post-printing processes (such as plasma treatment) were employed to reduce the contact angle of the surface to increase the adhesion of the damaged cells to the ROS scavenger thin film for their enhanced repair. A parameter-tunable inkjet printing method for the deposition of functional electronics materials that can simultaneously be used as ROS scavengers would enable to integrate bioelectronics for neural applications. Bioelectronic devices such as biosensors prepared with ROS scavenger materials can both monitor the cells' behavior as well as prevent cellular oxidative stress and DNA damage.

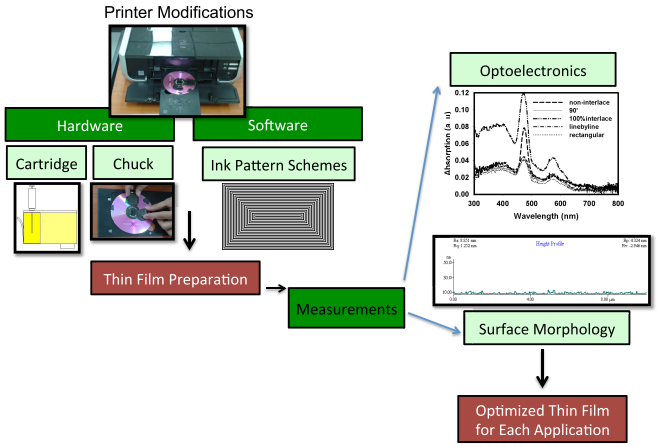

FIGURE 1. Thin film preparation includes: 1-Printer modification-Hardware and Software. 2-Thin film characterizations: Optoelectronics and Surface morphology.

II. MATERIALS AND METHODS

The first task in this work was to modify an ordinary inkjet printer to deposit thin films of functional materials with the ability to control the surface roughness of the films. Fig. 1 summarizes the procedures used to reengineer the hardware and software of an office printer. Optimized thin films, were obtained based on optoelectronic properties and surface morphology.

A. OFFICE PRINTER MODIFICATIONS

A commercial available PIXMA iP5300 color inkjet printer (Canon Inc.) capable of printing on the surface of compact discs (CDs) was used (Fig. 2a, b). This model is a drop-on-demand, thermal inkjet printer with a heater located on the side of the orifice (side-shooter) and five cartridges (black, pigment black, yellow, magenta, and cyan) (Fig. 2c, d). The commercial ink was drained using a small hole on the backside of the cartridge, the cartridge was washed using distilled water and dried with an air compressor and hairdryer. The cartridge was then refilled with organic ink (Fig. 2e-i).

For our purposes, we only filled the yellow-color cartridge with organic ink while the remaining cartridges contained distilled water to reduce the interaction of organic ink with its environment. The computer was programmed to print with the color "0, 0, 1, 0, 0" for black, pigment black, yellow, magenta, and cyan, respectively; this arrangement was optimal for preventing organic ink contamination. The set-up can be used for multifunctional device fabrications (e.g., solar cells or organic thin film transistors) when more number of organic materials are used in the device. In those cases, other cartridges can be filled with other materials and

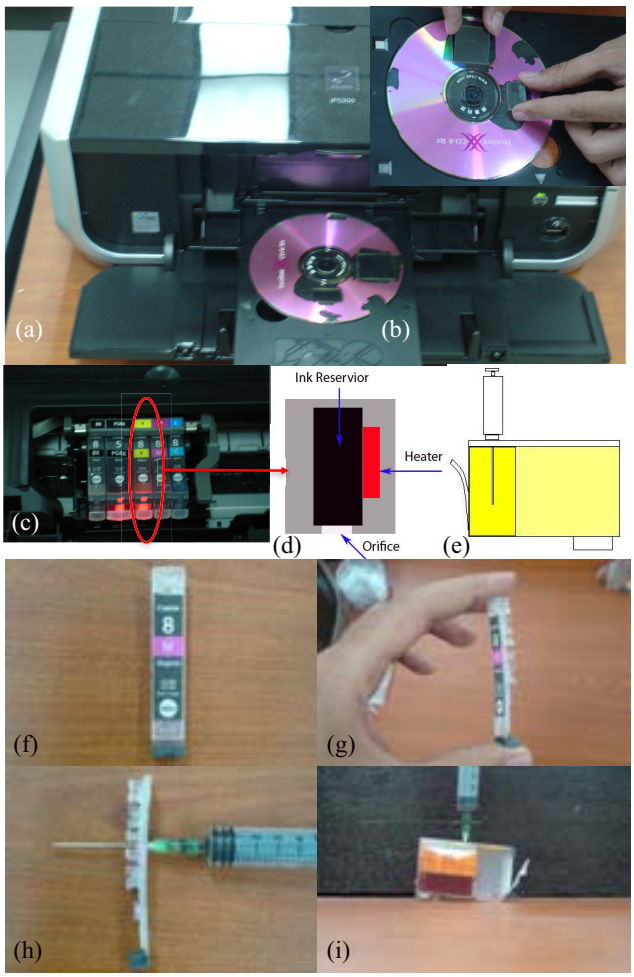

FIGURE 2. Modifying a thermal inkjet printer to deposit functional materials with the ability to control the surface on flexible and rigid substrates. (a) An office inkjet printer with the ability to print on a compact disc (CD). (b) A CD was used as a chuck to keep the substrate during the printing procedure. (c) This printer has five cartridges including black, pigment black, yellow, magenta, and cyan (d) Thermal cartridge (side shooter) has a heater attached to the ink reservoir to heat the ink and eject a droplet from the orifice. (e) The cartridge was cleaned using a syringe through a small entry in the backside of the cartridge. (f-i) the procedure to make a hole in backside of the cartridge for cleaning. The commercial ink was drained, the cartridge was washed with distilled water and dried using an air compressor and hairdryer. The cartridge was then filled with the functional material.

the color code can represent the appropriate organic ink to be printed.

One chuck was designed so that substrates were immobilized during the inkjet process. A CD was employed and was cut in two different places according to the sizes of the substrates (Fig. 2b). The printer software was programmed to print at the exact location of the substrates on the chuck. After printer modification, thin films with different characteristics were deposited to understand vital parameters of printed thin films.

Fabrication of organic electronic devices necessitates a versatile deposition modality to control the surface morphology of the films; nevertheless, the current deposition techniques rarely have this capability. To remedy this shortcoming, we tried to control the thin film properties with the modified printer.

During printing, drops can be placed in non-interlaced or interlaced schemes [29]. In a non-interlaced printing scheme, to cover the substrate totally, drops are placed consecutively and usually with some degree of overlap between two adjacent drops. In an interlaced printing scheme, two or more incomplete patterns are printed subsequently to complete each other and cover the substrate together. The difference occurs in the time allowed for the material to spread and dry before the next drop or line is printed. We designed and studied five printing patterns, including one non-interlaced and four interlaced schemes. The first pattern (Fig. 3a) is referred to as non-interlaced; the second (Fig. 3b) is referred to as rectangular; the third (Fig. 3c) is right-angled; the fourth (Fig. 3d) is line-by-line; and the final pattern (Fig. 3e) is referred to as 100% interlaced and includes four complimentary schemes. Each interlaced sample comprised a combination of at least two complementary designs (P_2-P_{11}), that were printed in two minute intervals subsequently, for drying the previous print as to minimize the overlap effect. In 100% interlaced pattern, shown in Fig. 3e, four complimentary patterns were printed subsequently in 2-minute intervals to prepare the thin films. In this case, rows are represented as "r" and columns are shown using "c". First, all points with coordinates of (odd rows, odd columns) were printed. This was followed by (odd r, even c), (even r, odd c), and finally (even r, even c) that completed the thin film preparation. For 12 mm × 20 mm substrates 42 rows and 70 columns were used. The surface morphologies of the printed thin films were studied using AFM, absorption spectra with UV-Vis, and emission spectra of the thin films with luminescence spectrophotometry.

B. THIN FILM DEPOSITION AND CHARACTERIZATIONS

The ink comprised of "manganese (III) 5, 10, 15, 20-tetra (4-pyridyl)-21H, 23H-porphine chloride tetrakis (methochloride)" (MnTPPCL). In this experiment, glass slides as substrate were cut into 25 mm × 25 mm sizes and were used for UV-Vis and luminescence spectrophotometer measurements; 12 mm × 20 mm substrates were used for atomic force microscopy (AFM) measurements. The glass substrates were cleaned with distilled water, acetone, and ethanol using an ultrasonic bath for 15 minutes each and were dried using nitrogen flow. To obtain the effect of ink concentration on the quality of the deposited thin films, three ink concentrations (4, 6, and 8 mg/mL) were tested. The morphology of thin films was studied using AFM (Veeco). A PerkinElmer LAMBDA 900 UV-Vis spectrophotometer as well as a luminescence LS 55 spectrometer were used to study the optical properties of thin films.

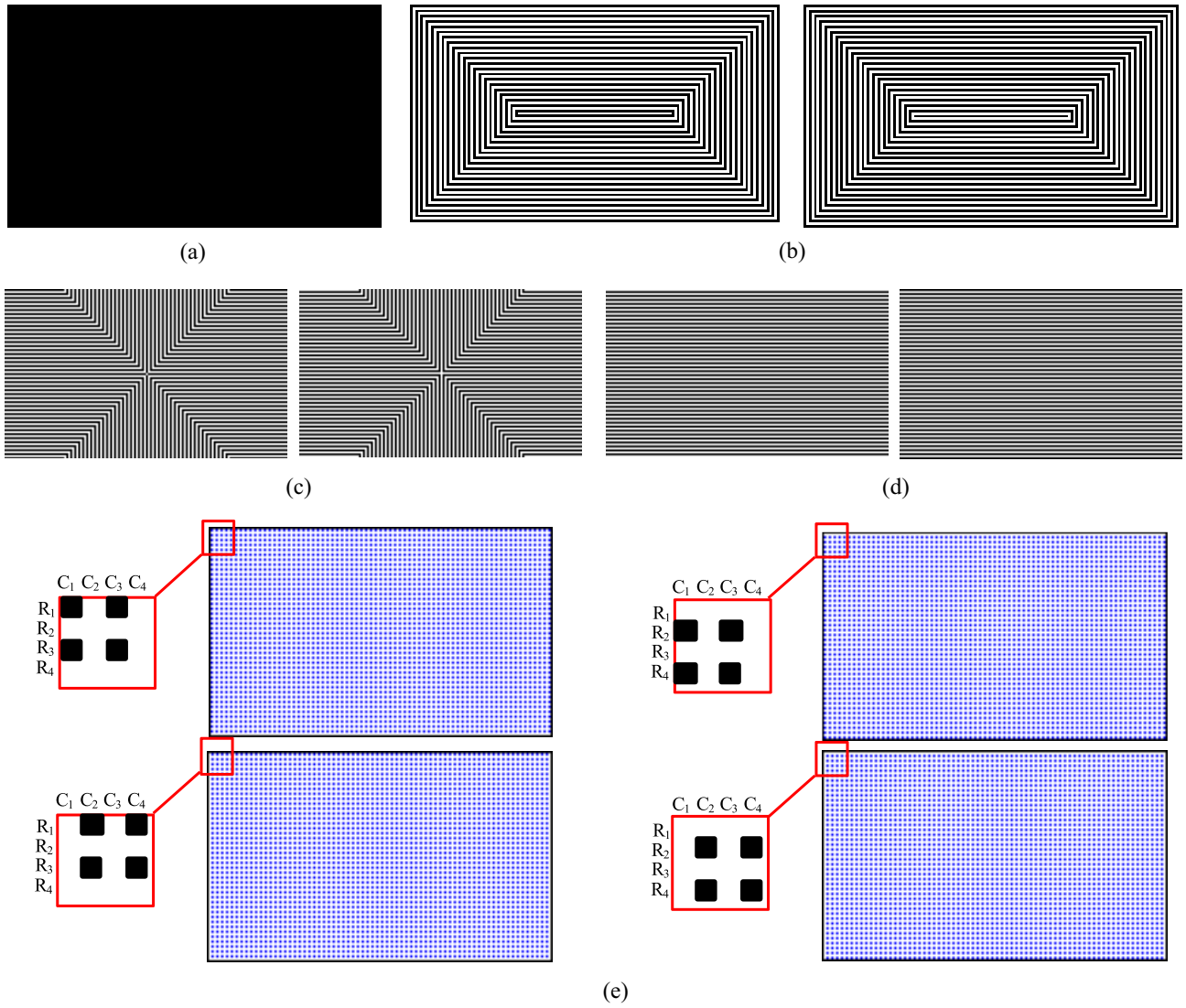

FIGURE 3. Different ink pattern schemes including interlaced and non-interlaced. (a) P_1 produces the non-interlaced pattern in which the droplets are printed consequently. (b) P_2 and P_3 are complementary designs for concentric rectangular. (c) P_4 and P_5 are the twins for producing the right angles pattern. (d) P_6 and P_7 are complementary designs for line by line pattern. (e) P_8-P_{11} the complementary designs for 100% interlaced pattern. In each complementary pattern scheme, different columns (C) and rows (R) are printed. In this case, P_8 prints on R_{odd} and C_{odd}, P_9 prints on C_{even} and R_{odd}, P_{10} prints on C_{odd} and R_{even}, and finally P_{11} prints on C_{even} and R_{even} that completes the printing procedure to cover the surface totally. Each pattern comes in a time interval delay that lets the previous droplets get dried–decreasing the amount of overlap.

C. FUNCTIONALIZING THE INKJET-PRINTED FILMS OF ROS SCAVENGER/ELECTRONIC MATERIAL FOR CELL CULTURING

In order to enhance the effect of ROS scavenger material on neural resilience the interface of cell/material plays a critical role. It has been shown that surface characteristics are very important for adhesion, differentiation, and proliferation of cells [4]. By changing the wettability one can control the cellular function and surface interactions on thin films. To provide a reliable attachment between cells and inkjet-printed thin films as the culturing surface, the inkjet-printed films were treated after the printing procedure using 45 seconds with medium power using a plasma cleaner PDC-32G (Harrick Plasma, Ithaca, NY, USA). The process changed the wettability of the surface that helps the cells attach to the inkjet-printed films to communicate with ROS scavenger/electronic materials.

III. RESULTS AND DISCUSSION

First, the optimal concentration of ink was determined by comparing the optical absorption of three different concentrations of thin films. In this part, all thin films were using non-interlaced ink pattern scheme. UV-Vis (Fig. 4) indicated that an ink concentration of 6 mg/mL produced a thin film with the highest absorption spectra; we used this concentration going forward.

The surface morphologies of all the thin films, prepared with different patterns, were studied using AFM to evaluate

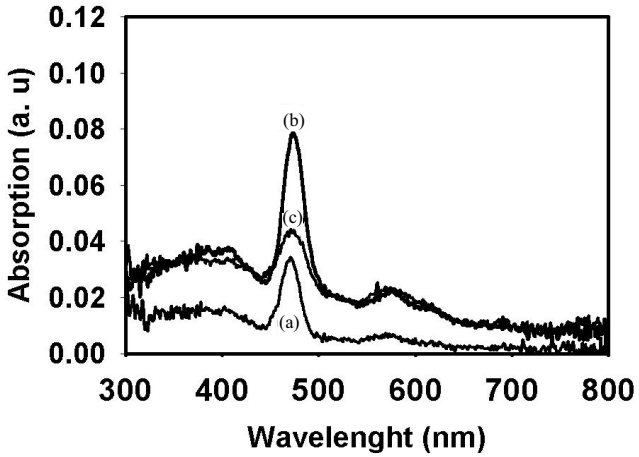

FIGURE 4. **Absorption spectra for three different concentrations, (a) 4 mg/mL, (b) 6 mg/mL, and (c) 8 mg/mL.**

the different degrees of overlap in terms of the various ink pattern schemes, while the absorption and emission spectra of the thin films were also analyzed to compare the optical parameters of the samples.

Photoluminescence measurements Fig. 5a confirmed that the emission spectra did not change with various number of layers (except for intensity), indicating that the chemical properties did not change. The peak in emission spectra shows in 630 nm (∼1.96 eV). Moreover, Fig. 5b shows the comparison between the absorption spectra of the thin films. The forms, curves, and positions of the peaks of the spectra were almost the same for all films. However, the curves showed dissimilar intensities; the film using the 100% interlaced pattern had the highest absorption intensity. The absorption spectra show a main peak in 480 nm (∼2.5 eV) and two weaker absorption peak in 590 nm (∼2.1 eV) and 410 nm (∼3.02 eV).

Fig. 6 shows AFM-height profiles of two inkjet-printed films prepared with two different pattern schemes. It indicates that the 100% interlaced pattern is much smoother than the non-interlaced counterpart, which is related to the printing process. In the non-interlaced printing, each drop of ink overlaps with neighbor drops at its edges, thus producing higher peaks at the edges of the drops and valleys in their centers. These peak and valley formations eventually increase the surface roughness (Fig. 6). Contrary to the non-interlaced pattern, each drop in the 100% interlaced printing has less overlap with previous drops (that had been dried) owing to the delay in printing adjacent droplets, thus making the thin film smoother. AFM confirmed the ability of this deposition modality to control the surface roughness of prepared thin films. To our knowledge, this is the most reliable deposition technique with the ability to control the surface roughness of thin films. In electronic device fabrication, controlling the surface roughness may enhance the device performance dramatically.

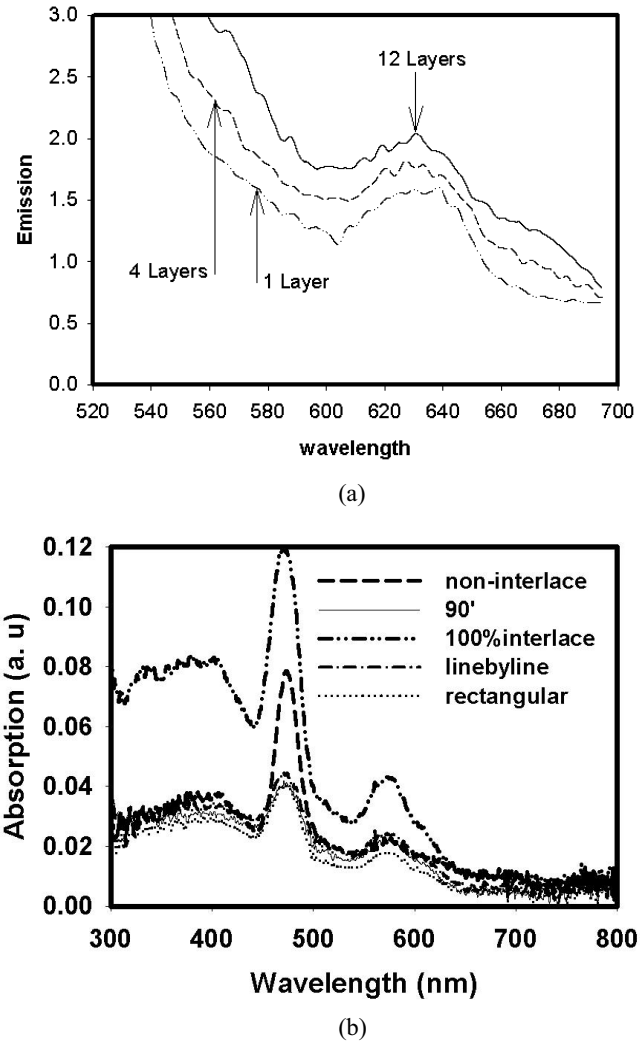

FIGURE 5. **(a) Emission spectra for different number of layers show consistent peaks, (b) Absorption spectra for all the different patterns with the same concentrations.**

TABLE 1. **Surface roughness of different inkjet-printed films with different ink pattern schemes.**

Ink Pattern Schemes	Average Film Roughness (nm)
Non-interlaced	41.20
Right angles	11.90
Line by line	10.49
100% Interlace	8.85
Rectangular	8.84

Different ink pattern schemes applied in inkjet printing of a ROS scavenger/electronics functional material and the resulted films' roughness determined by atomic force microscopy. The average surface roughness was tuned using different designed innovative schemes ranging from 8.84 to 41.20 nm.

Table 1 indicates that the films printed with the non-interlaced scheme showed the highest average roughness among all of the printed films. Nevertheless, thin films printed with 100% interlaced and rectangular schemes

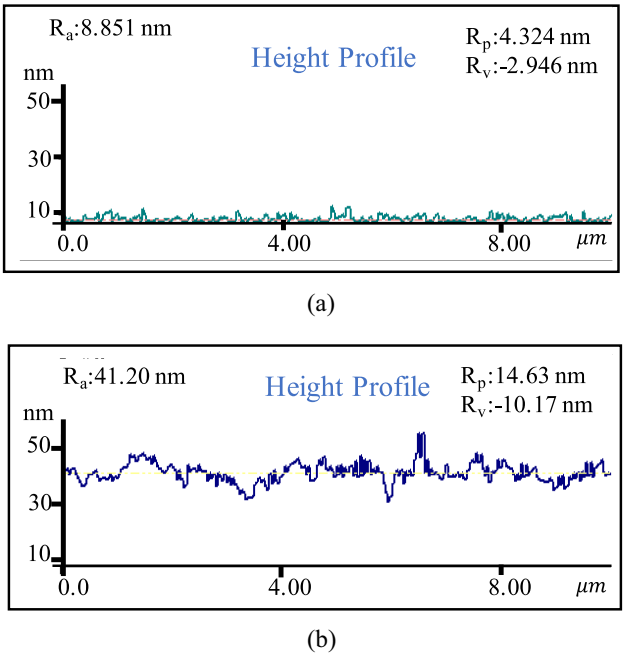

FIGURE 6. **Height profile of thin films based on Atomic Force Microscopy (AFM) results for (a) 100% interlaced. Films showed average roughness 8.85 nm with maximum profile peak height 4.32 nm and maximum valley depth in −2.94 resulting in a peak to valley equal to 7.26 nm, and (b) non-interlaced scheme. Films showed average roughness 41.20 nm with maximum profile peak height 14.63 nm and maximum valley depth in −10.17 nm resulting in a peak to valley equal to 24.8 nm. This height profile comparison confirms smoother surface for films prepared with interlaced ink pattern schemes.**

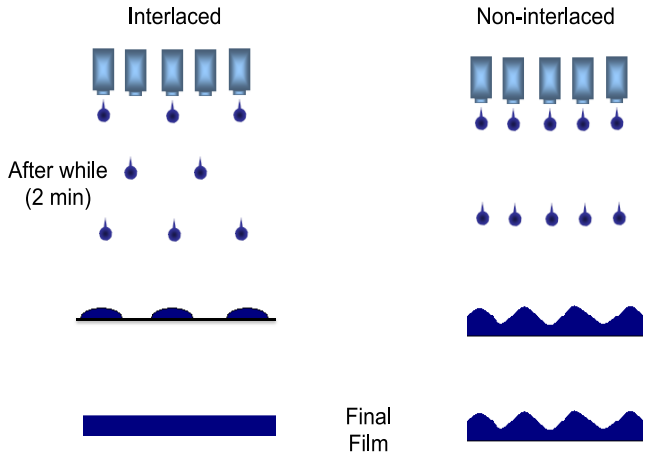

FIGURE 7. **The difference between interlaced and non-interlaced schemes: In non-interlaced schemes the drops are printed subsequently and have some amount of overlap. Therefore, they provide films with a higher surface roughness that can be used to fabricate organic sensors. In the interlaced scheme, however, the formerly printed drops have a short time to rest on the surface and dry before the later drops are printed. In this case, the neighboring droplets encounter minimum overlap and provide smoother thin films that are favorable for organic solar cell and organic light-emitting diodes applications.**

demonstrated the smoothest surface compared to other films. These results, in addition to the information from the absorption spectra, served as useful guidelines for selecting the appropriate thin films for specific applications. Our final determination that the highest absorption spectrum was attained by using the 100% interlaced film indicates that this pattern scheme is ideal for printing smooth thin films. Applications for this include the fabrication of organic solar cells and organic light-emitting diodes where smooth films increase the charge transformation in the device. On the other hand, for other applications, such as fabricating the organic gas sensors in which a higher degree of roughness provides a greater surface area to trap gas molecules, the non-interlaced pattern is more suitable for depositing the appropriate film. For bio-related applications like transistor-based biosensor preparation, smooth films are needed to fabricate high-quality transistors that can be functionalized using different agents for specific bioanalytes.

Fig. 7 elucidates the concept of interlaced schemes by comparing the discrepancies between printing of interlaced and non-interlaced patterns as well as the effect of overlapping drops on tuning the surface roughness of the films.

The cells are sensitive to the surface if the surface energy is not optimized and wettability is low. The wettability of the surface is important for cellular interactions [4]. Therefore, the contact angle (relevant to the surface energy) was optimized for the inkjet-printed films. Cells may show minimum attachment to untreated films; however, this was addressed using plasma-cleaning treatment of the inkjet-printed films following the printing procedure and prior to cell culturing. The lower contact angle shows higher surface energy and wettability. For the purpose of fabricating electronic devices on which cell culturing is feasible, it is important to consider the surface roughness when measuring the contact angle. As stated by Wenzel in 1936, the surface roughness influences the contact angle and wettability of a specific surface [30]. It was shown that

$$A = S_1 - S_{12} = S_2 \cos\theta \tag{1}$$

where A, S_1, S_{12}, S_2, and θ denote adhesion tension, specific energy of the interface before wetting, specific energy of the interface after wetting, surface tension of the liquid, and contact angle respectively. Using a roughness factor "r" as the ratio of actual surface to geometric surface Wenzel showed

$$rA = r(S_1 - S_{12}) = S_2 \cos\theta \tag{2}$$

where r is equal to 1 for smooth surfaces and is always more than 1 for rough surfaces. In this case, rA is called effective adhesion tension that can be measured experimentally. During surface wetting the free liquid surface increases and needs energy. The speed of wetting is determined by the difference in the net energy. Therefore, for the same increase in the free liquid area at the upper surface of the drop a greater surface can be wet when it is rough. For the rough surface to induce the spreading a drop there is a greater net energy decrease and the rough surface can be wet more rapidly [30].

This shows that the contact angle for a rough surface is always smaller than that in a smooth surface, and confirms our results that the smoother films needed longer treatments to optimize the angle. However, in this case, smoother films are more favorable owing to the fact that the films might be used for electronic device fabrication prior to cell culturing. We treated films with different plasma powers and durations to decrease the contact angle and thereby enable cell attachment. The minimum Plasma exposure was found 45 seconds under medium power to achieve cell/material interface. In this paper, we concentrated on printing functional materials and surface morphology, as the future of the work more surface treatment can be performed using extracellular matrix proteins such as collagen. Collagen is one of the abundant proteins in the body and has the ability to promote the attachment of cells to the inkjet-printed films.

IV. CONCLUSION

Reactive oxygen species (ROS) can damage neural cells due to oxidative stress. This can cause many acute or chronic diseases. ROS scavenger agents, on the other hand, are excellent material candidates for neural resilience. Integrating electronic devices such as biosensors into cellular systems can help monitor and control the 2- or 3-dimensional biological structures. Fabrication of biocompatible electronic devices with functional electronic materials that shows ROS scavenger behaviors can introduce a new research strategy in neural studies. To optimize the deposition procedure, a deposition modality was devised to control the surface morphology of the thin films. An office inkjet printer was modified in a way to control the properties of the organic thin films. Using a computer-assisted deposition process, interlaced and non-interlaced ink patterns were printed and successfully deposited thin films with a wide range of surface roughness. It is worth noting that the difference in surface roughness with different printing schemes is dependent on the variance of the overlapping drops. The inkjet-printed films were treated post-printing with the optimum surface energy that would allow cells to attach to the surface. The inkjet printed material has both ROS scavenger behaviors and electronic properties. The integration of flexible bioelectronic devices with cellular systems and employing the ROS scavenger properties may allow for the recovery of damaged cell functionality while monitoring them using biocompatible electronic devices. In the future, we can envision fabrication of biosensors and other biocompatible electronic devices that can be used for detecting different biomarkers in the biological systems while they have repairing properties for the damaged cells. This can be a new era of functional electronic and functional biological device fabrication with low-cost deposition technique with surface roughness curb.

ACKNOWLEDGMENT

The authors would like to thank Drs. Jareer Kassis and Rongyuan Xie for fruitful discussions.

REFERENCES

[1] J.-L. Yang, P. Sykora, D. M. Wilson, M. P. Mattson, and V. A. Bohr, "The excitatory neurotransmitter glutamate stimulates DNA repair to increase neuronal resiliency," *Mech. Ageing Develop.*, vol. 132, no. 8, pp. 405–411, Sep. 2011.

[2] J.-L. Yang, T. Tadokoro, G. Keijzers, M. P. Mattson, and V. A. Bohr, "Neurons efficiently repair glutamate-induced oxidative DNA damage by a process involving CREB-mediated up-regulation of apurinic endonuclease 1," *J. Biol. Chem.*, vol. 285, no. 36, pp. 28191–28199, Sep. 2010.

[3] M. Elżbieciak-Wodka and P. Warszyński, "Effect of deposition conditions on thickness and permeability of the multilayer films formed from natural polyelectrolytes," *Electrochimica Acta*, vol. 104, pp. 348–357, Aug. 2013.

[4] G. Scarpa, A. L. Idzko, S. Götz, and S. Thalhammer, "Biocompatibility studies of functionalized regioregular poly(3-hexylthiophene) layers for sensing applications," *Macromol. Biosci.*, vol. 10, no. 4, pp. 378–383, Apr. 2010.

[5] A. Shafiee, E. Ghadiri, J. Kassis, N. P. Zarandi, and A. Atala, "Biosensing technologies for medical applications, manufacturing, and regenerative medicine," *Current Stem Cell Rep.*, vol. 4, no. 2, pp. 105–115, Apr. 2018.

[6] F. C. Krebs, "Fabrication and processing of polymer solar cells: A review of printing and coating techniques," *Solar Energy Mater. Solar Cells*, vol. 93, no. 4, pp. 394–412, Apr. 2009.

[7] A. Shafiee, M. M. Salleh, and M. Yahaya, "Fabrication of organic solar cells based on a blend of donor-acceptor molecules by inkjet printing technique," in *Proc. IEEE ICSE*, Johor Bahru, Malaysia, 2008, pp. 319–322.

[8] A. Shafiee, M. M. Salleh, and M. Yahaya, "Fabrication of organic solar cells based on a blend of poly (3-octylthiophene-2, 5-diyl) and fullerene derivative using inkjet printing technique," in *Proc. SPIE*, vol. 7493. Weihai, China, 2009, Art. no. 74932D.

[9] W. Z. Samad, M. M. Salleh, A. Shafiee, and M. A. Yarmo, "Preparation nanostructure thin films of fluorine doped tin oxide by inkjet printing technique," in *Proc. AIP Conf.*, vol. 1284. Bandung, Indonesia, 2010, pp. 83–86.

[10] W. Z. Samad, M. M. Salleh, A. Shafiee, and M. A. Yarmo, "Transparent conducting thin films of fluoro doped tin oxide (FTO) deposited using inkjet printing technique," in *Proc. IEEE ICSE*, Melaka, Malaysia, 2010, pp. 52–55.

[11] W. Z. Samad, M. M. Salleh, A. Shafiee, and M. A. Yarmo, "Transparent conductive electrode of fluorine doped tin oxide prepared by inkjet printing technique," *Mater. Sci. Forum*, vols. 663–665, pp. 694–697, Nov. 2010.

[12] R. D. Boehm, P. R. Miller, J. Daniels, S. Stafslien, and R. J. Narayan, "Inkjet printing for pharmaceutical applications," *Mater. Today*, vol. 17, no. 5, pp. 247–252, Jun. 2014.

[13] A. Shafiee, M. McCune, G. Forgacs, and I. Kosztin, "Post-deposition bioink self-assembly: A quantitative study," *Biofabrication*, vol. 7, no. 4, Oct. 2015, Art. no. 045005.

[14] M. Mccune, A. Shafiee, G. Forgacs, and I. Kosztin, "Predictive modeling of post bioprinting structure formation," *Soft Matter*, vol. 10, no.11, pp. 1790–1800, Mar. 2014.

[15] A. Shafiee, C. Norotte, and E. Ghadiri, "Cellular bioink surface tension: A tunable biophysical parameter for faster maturation of bioprinted tissue," *Bioprinting*, vol. 8, pp. 13–21, Dec. 2017.

[16] A. Shafiee, E. Ghadiri, D. Williams, and A. Atala, "Physics of cellular self-assembly—A microscopic model and mathematical framework for faster maturation of bioprinted tissues," *Bioprinting*, vol. 14, 2019, Art. no. e00047. [Online]. Available: https://doi.org/10.1016/j.bprint.2019.e00047

[17] C. J. Ferris, K. G. Gilmore, G. G. Wallace, and M. I. H. Panhuis, "Biofabrication: An overview of the approaches used for printing of living cells," *Appl. Microbiol. Biotechnol.*, vol. 97, no. 10, pp. 4243–4258, May 2013.

[18] A. Shafiee, M. M. Salleh, and M. Yahaya, "Determination of HOMO and LUMO of [6,6]-Phenyl C_{61}-butyric acid 3-ethylthiophene ester and poly (3-octyl-thiophene-2, 5-diyl) through voltametry characterization," *Sains Malaysiana*, vol. 40, no. 2, pp. 173–176, Feb. 2011.

[19] T. W. Kelley *et al.*, "Recent progress in organic electronics: Materials, devices, and processes," *Chem. Mater.*, vol. 16, no. 23, pp. 4413–4422, Nov. 2004.

[20] W. Z. Samad, M. M. Salleh, A. Shafiee, and M. Yahaya, "Structural, optical and electrical properties of fluorine doped tin oxide thin films deposited using inkjet printing technique," *Sains Malaysiana*, vol. 40, no. 3, pp. 251–257, 2011.
[21] E. Ghadiri, N. Taghavinia, H. R. Aghabozorg, and A. I. Zad, "TiO_2 nanotubular fibers sensitized with CdS nanoparticles," *Eur. Phys. J. Appl. Phys.*, vol. 50, no. 2, May 2010, Art. no. 20601.
[22] C. Bauer *et al.*, "Dynamics and mechanisms of interfacial photoinduced electron transfer processes of third generation photovoltaics and photocatalysis," *Chimia Int. J. Chem.*, vol. 65, no. 9, pp. 704–709, Sep. 2011.
[23] E. Ghadiri, D. Shin, A. Shafiee, W. S. Warren, and D. B. Mitzi, "Grain-resolved ultrafast photophysics in $Cu_2BaSnS_{4-x}Se_x$ semiconductors using pump-probe diffuse reflectance spectroscopy and microscopy," *ACS Appl. Mater. Interfaces*, vol. 10, no. 46, pp. 39615–39623, Oct. 2018.
[24] H. E. Katz and J. Huang, "Thin-film organic electronic devices," *Annu. Rev. Mater. Res.*, vol. 39, pp. 71–92, Aug. 2009.
[25] J. M. D'Arcy *et al.*, "Versatile solution for growing thin films of conducting polymers," *Proc. Nat. Acad. Sci. USA*, vol. 107, no. 46, pp. 19673–19678, Nov. 2010.
[26] B. Derby, "Bioprinting: InkJet printing proteins and hybrid cell-containing materials and structures," *J. Mater. Chem.*, vol. 18, no. 47, pp. 5717–5721, Dec. 2008.
[27] P. Calvert, "Inkjet printing for materials and devices," *Chem. Mater.*, vol. 13, no. 10, pp. 3299–3305, Oct. 2001.
[28] H. P. Le, "Progress and trends in ink-jet printing technology," *J. Imag. Sci. Technol.*, vol. 42, pp. 49–62, Jul. 1998.
[29] V. G. Shah and D. B. Wallace, "Low-cost solar cell fabrication by drop-on-demand inkjet printing," in *Proc. 37th Annu. Int. Symp. Microelectron. (IMAPS)*, Nov. 2004, pp. 1–6.
[30] R. N. Wenzel, "Resistance of solid surfaces to wetting by water," *Ind. Eng. Chem.*, vol. 28, no. 8, pp. 988–994, Aug. 1936.

ASHKAN SHAFIEE received the B.Sc., M.Sc., and Ph.D. degrees in physics and the M.Sc. degree in microengineering and nanoelectronics. He has been researching on optoelectronics, printed electronics, and bioprinting since 2000. His research expands from bioprinting and organ fabrication to printing of biocompatible and degradable electronic devices and their applications in regenerative medicine.

ELHAM GHADIRI is an expert in nanotechnology, nanomaterial/nano-device fabrication and ultrafast laser spectroscopy/microscopy. She is an Assistant Professor with Wake Forest University, USA. Her research interests expand from functional electronic material fabrication to integration of ultrafast laser techniques for fundamental photochemical dynamics characterizations. She performed her Ph.D. thesis and post-doctoral training under the supervision of eminent experts M. Gratzel, J. Moser, and W. S. Warren with EPFL, Switzerland, and Duke University, USA.

MUHAMAD MAT SALLEH received the Ph.D. degree in solid state physics from the University of London, U.K., in 1979. His research interests lay in organic electronics and organic device fabrication. He is a Professor with the Institute of Microengineering and Nanoelectronics, National University of Malaysia.

MUHAMMAD YAHAYA received the Ph.D. degree in physics from Monash University, Australia. He is an emeritus Professor with the Institute of Microengineering and Nanoelectronics, National University of Malaysia. He is an expert in sensors, solar energy, thin film deposition, and material study.

ANTHONY ATALA is the Director of the Wake Forest Institute for Regenerative Medicine, Wake Forest University, NC, USA. His research areas of interest include stem cells, tissue engineering, and regenerative medicine.